

A Study of Dirac Fermionic Dark Matters

Chun-Khiang Chua, Ron-Chou Hsieh

Department of Physics and Chung Yuan Center for High Energy Physics,

Chung Yuan Christian University,

Chung-Li, Taiwan 320, Republic of China

Abstract

We study pure weak eigenstate Dirac fermionic dark matters (DM). We consider WIMP with renormalizable interaction. According to results of direct searches and the nature of DM (electrical neutral and being a pure weak eigenstate), the quantum number of DM is determined to be $I_3 = Y = 0$. There are only two possible cases: either DM has non-vanishing weak isospin ($I \neq 0$) or it is an isosinglet ($I = 0$). In the first case, the Sommerfeld enhancement is sizable for large I , producing large $\chi^0 \bar{\chi}^0 \rightarrow VV$ rates. In particular, we obtain large $\chi \bar{\chi} \rightarrow W^+ W^-$ cross section, which is comparable to the latest bounds from indirect searches and m_χ is constrained to be larger than few hundred GeV to few TeV. It is possible to give correct relic density with m_χ higher than these lower bounds. In the second case, to couple DM to standard model (SM) particles, a SM-singlet vector mediator X is required from renormalizability and the SM gauge quantum numbers. To satisfy the latest bounds of direct searches and to reproduce the DM relic density at the same time, resonant enhancement in DM annihilation diagram is needed. Thus, the masses of DM and the mediator are related. Furthermore, this model is not sufficient to explain the deviation in muon $g - 2$.

I. INTRODUCTION

It is known that the discrepancy in speed of galaxy in our universe between observation and prediction from Newtonian gravitation theory indicate that there must be something “dark” there. These so called dark matter (DM), according to the observation of Wilkinson Microwave Anisotropy Probe (WMAP) and Planck, supply about 23% of composition to our universe [1, 2]. Dark matter cannot be observed from measuring their luminosity. Then, would it be possible that they are something like black hole, neutral star, brown dwarf, etc., which can only emit little or even no electro-magnetic radiation. Big-Band nucleosynthesis (BBN) provides powerful constraints on this account. From predictions of the abundances of the light elements, D, ^3He , ^4He , etc., one can evaluate the value of relic blackbody photon density as $\eta \equiv n_b/n_\gamma \approx (5.1 - 6.5) \times 10^{-10}$ [3]. The measurements can be converted to the baryonic fraction of critical density, $\Omega_b = \rho_b/\rho_{\text{crit}} \simeq (0.019 - 0.04)h^{-2}$, where $h = 0.72 \pm 0.08$ is the present Hubble parameter. The resulting baryonic fraction Ω_b is much smaller than the latest result on cold DM fraction, $\Omega_{\text{DM}}h^2 = 0.1187 \pm 0.0017$ [2]. It tells us that, in the standard model (SM) of particle physics, there is no candidate for DM. Therefore, one has to extend the SM to account for the DM.

To construct a DM model, there are some basic requirements on DM. DM must be stable, charge neutral and have non-negligible mass. “Stable” means that it should live long enough that we can still observe their relic. “Neutral” is to avoid DM to shine and “non-negligible mass” means that the DM can gather gravitationally on small scales and so seed galaxy formation. There are many DM candidates such as weakly interactive massive particles (WIMP), axions, Kaluza-Klein mode in extra dimensions, etc.. For a recent review of dark matter, see [4].

In this study, we will only consider the WIMP scenario. DM only interact through the gravity and weakly interacting force with interaction cross-sections basically not higher than the weak scale. We investigate a renormalizable DM model by introducing a pure weak eigenstate Dirac fermion as a DM candidate. We do not consider scalar or Majorana DM, which have been discussed intensively in the literature (see, for example, [5–11]). There are some Dirac fermionic DM models being considered in past years [12–17]. For instance, fermionic DM contributing to indirect precesses [12, 13], fermionic DMs with a charged scalar particle as a mediator to couple to SM particles through renormalizable terms are discussed in [14], while some use vector bosons, such as Z' , to mediate interactions with SM particles [15–17]. In this work the models we considered are viewed as purely low energy models. The UV completion of the models is beyond the scope of the present work.

The lay out of this work is as following. In the next section, we introduce a weak eigenstate Dirac fermionic DM model with renormalizable interaction. We try to develop the model logically with a bottom-up approach. We then constrain the model using relic density, direct and indirect detection experiments. Numerical results are presented in Sec. III, which follows by discussion and conclusion in Sec. IV. Some formulas are collected in the Appendix.

II. FRAMEWORK

In WIMP scenario one can write down a simple DM model by adding on SM a single Dirac fermionic multiplet χ with the Lagrangian such as: [18]

$$\mathcal{L} = \mathcal{L}_{\text{SM}} + \bar{\chi}(i\not{D} - m_\chi)\chi, \quad (1)$$

where the covariant derivative D_μ contains the known electroweak gauge couplings to the vector bosons of the SM such that

$$\begin{aligned} D_\mu &= \partial_\mu + i\frac{g}{\sqrt{2}}(W_\mu^+T^+ + W_\mu^-T^-) + i\frac{1}{\sqrt{g^2 + g'^2}}Z_\mu(g^2T^3 - g'^2Y) + i\frac{gg'}{\sqrt{g^2 + g'^2}}A_\mu Q \\ &= \partial_\mu + i\frac{g}{\sqrt{2}}(W_\mu^+T^+ + W_\mu^-T^-) + i\frac{g}{\cos\theta_W}Z_\mu T^3. \end{aligned} \quad (2)$$

Here, in the second line we have used the condition ‘‘electric charge neutrality’’, $Q = T^3 + Y = 0$, and the definition of weak mixing angle, $\cos\theta_W = g/\sqrt{g^2 + g'^2}$. Note that in this work we only consider renormalizable interactions. Therefore, the DM cannot couple to Higgs. Furthermore, we may assign some Z_2 symmetry to maintain the stability of the DM.

In the Lagrangian, the Z boson interaction term will produce a tree-level spin independent elastic cross sections with a nucleus N :

$$\sigma_A^{\text{SI}}(\chi N \rightarrow \chi N) = \frac{\mu_N^2}{4\pi} \left(\frac{g}{\cos\theta_W M_Z} \right)^4 I_3^2 \left[-\frac{1}{4}(A - Z) + \left(\frac{1}{4} - \sin^2\theta_W \right) Z \right]^2, \quad (3)$$

where Z and A are the number of protons and of nucleons in the target nucleus, I_3 is the weak isospin quantum number and μ_N is the reduce mass of DM and nucleus. The above formula gives a normalized cross section (see Appendix A)

$$\sigma_N^Z \simeq I_3^2 \times 10^{-40} \text{cm}^2, \quad (4)$$

for m_χ ranges from few GeV to few TeV. ¹ Therefore, the magnitude of the cross section exceeds most of the experimental upper bounds which obtained from direct detection searches for $m_\chi \gtrsim 10$ GeV [20].² The situation forces us to consider two cases of heavy DM with different quantum numbers: (i) $I \neq 0, I_3 = Y = 0$, and (ii) $I = Y = 0$.

Before we proceed to these two cases, it will be useful to recall some basics formulas. To obtain the thermal relic density for DM, we must solve the Boltzmann equation, which control the evolution of the DM abundance,

$$\frac{dn_\chi}{dt} + 3Hn_\chi = -\langle\sigma_{\text{ann}}v\rangle_{\chi\bar{\chi}}[n_\chi n_{\bar{\chi}} - n_\chi^{\text{eq}} n_{\bar{\chi}}^{\text{eq}}], \quad (5)$$

where $H \equiv \dot{a}/a = \sqrt{4\pi^3 g_*(T) T^4 / (45 M_{\text{PL}}^2)}$ is the Hubble parameter, M_{PL} is the Planck mass, g_* is the total effective numbers of relativistic degrees of freedom [22, 23], $\langle\sigma_{\text{ann}}v\rangle_{\chi\bar{\chi}}$ is the thermal averaged $\chi\bar{\chi}$ annihilation cross section and $n_\chi(n_{\bar{\chi}})$ is the number density of DM (anti-DM). Note

¹ The mass of the fermionic DM should be larger than GeV, which is known as the Lee-Weinberg limit [19].

² In fact, the case of DM with non-vanishing T_3 is still allowable for light WIMP candidates by only consider the constraint from direct detection searches. There are also some efforts are devoted to searching for DM with mass of order $\lesssim 10$ GeV [21]. But, here we do not consider light DM case.

that for the Dirac fermionic DM, we have $n_{DM} = n_\chi + n_{\bar{\chi}} = 2n_{\chi(\bar{\chi})}$ for the DM number density, and, consequently, we obtain

$$\frac{dn_{DM}}{dt} + 3Hn_{DM} = -\frac{\langle\sigma_{\text{ann}}v\rangle_{\chi\bar{\chi}}}{2} \left[n_{DM}^2 - (n_{DM}^{\text{eq}})^2 \right] = -\langle\sigma_{\text{ann}}v\rangle \left[n_{DM}^2 - (n_{DM}^{\text{eq}})^2 \right], \quad (6)$$

where we define $\langle\sigma_{\text{ann}}v\rangle \equiv \langle\sigma_{\text{ann}}v\rangle_{\chi\bar{\chi}}/2$, such that the Boltzmann equation can take the usual form. The physical reasoning of the factor 1/2 can be understood as following. DM can be separated into two halves (χ and $\bar{\chi}$). Half of the DM (χ or $\bar{\chi}$) can only annihilate with the other half of the DM ($\bar{\chi}$ or χ) and vice versa, giving factor 1/4 each. Therefore, by adding these two halves, we obtain the factor 1/2. We note in passing that $DM + N$ elastic scattering cross section, does not need the factor 1/2, since it is compensated by a factor 2 arisen from $\chi + N$ and $\bar{\chi} + N$ scatterings.

Following the standard procedure [22] to solve Eq.(5) approximately, we obtain the relations:

$$\Omega_{\text{DM}}h^2 \approx 1.04 \times 10^9 \frac{\text{GeV}^{-1}}{M_{\text{PL}}\sqrt{g_*(T_f)}J(x_f)}, \quad (7)$$

$$x_f \approx \ln \left[\frac{2 \times 0.038 m_\chi M_{\text{PL}} \langle\sigma_{\text{ann}}v\rangle}{\sqrt{g_*(T_f)} x_f^{1/2}} \right], \quad (8)$$

where we have

$$J(x_f) \equiv \int_{x_f}^{\infty} \frac{\langle\sigma_{\text{ann}}v\rangle}{x^2} dx \quad (9)$$

with x_f defined as m_χ/T_f and T_f being the freeze-out temperature, and the thermal averaged annihilation cross section $\langle\sigma_{\text{ann}}v\rangle$ with v the ‘‘relative velocity’’ is defined as

$$\begin{aligned} \langle\sigma_{\text{ann}}v\rangle &\equiv \frac{\langle\sigma_{\text{ann}}v\rangle_{\chi\bar{\chi}}}{2} \equiv \frac{3\sqrt{6}}{\sqrt{\pi}v_0^3} \int_0^\infty dv v^2 \frac{\langle\sigma_{\text{ann}}v\rangle_{\chi\bar{\chi}}}{2} e^{-3v^2/2v_0^2} \\ &= \frac{x^{3/2}}{2\sqrt{\pi}} \int_0^\infty dv v^2 \frac{\langle\sigma_{\text{ann}}v\rangle_{\chi\bar{\chi}}}{2} e^{-xv^2/4}, \end{aligned} \quad (10)$$

where we define $v_0 \equiv \langle v^2 \rangle^{1/2}$ and $v_0 = \sqrt{6/x_f}$ has been used in the last expression. It is straightforward to obtain

$$J(x_f) = \int_{x_f}^{\infty} \frac{\langle\sigma_{\text{ann}}v\rangle}{x^2} dx = \int_0^\infty dv \frac{(\sigma v)_{\chi\bar{\chi}}}{2} v \left[1 - \text{erf} \left(v\sqrt{x_f}/2 \right) \right]. \quad (11)$$

Note that in the above equations factors of 1/2 arisen from $n_{DM} = n_\chi + n_{\bar{\chi}} = 2n_{\chi(\bar{\chi})}$ are included. We can now turn to the formalisms for the two above mentioned cases.

I. $\mathbf{I} \neq 0, \mathbf{I}_3 = \mathbf{Y} = 0$ case

In this case, the DM possesses non-vanishing weak isospin I but with zero hypercharge. The constraint condition, $I_3 = 0$, indeed avoids the troublesome Z diagram. However, the contribution from the W boson interaction needs to be investigated as well. Note that this case was also studied in [18, 24]. For completeness, we shall include them in this analysis. In fact, this work differs from the previous studies in several aspects. We focus on the Dirac Fermionic DM case. We are interested in finding the direct consequences of Eq. (1) instead of completing the model by

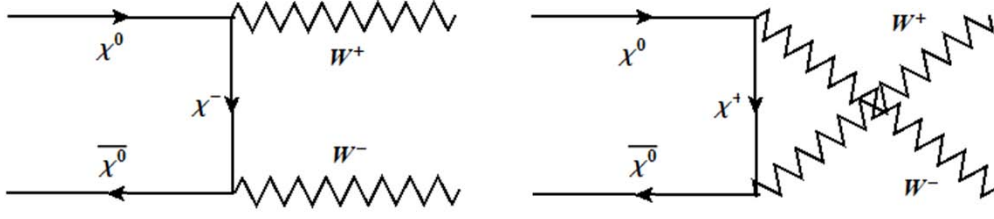


FIG. 1: The Feynman diagrams of DM annihilation for W^+W^- channel.

adding other ingredients. Therefore, all isospin assignments are kept. As we will discuss later, the Sommerfeld effects applicable to any isospin assignment will also be given. Furthermore, we are in a position that new data, such as galactic annihilation rate [25], is available and can be compared to.

The DM pair can annihilate into a W boson pair (see Fig. 1) and then can contribute to the relic density of DM and indirect processes from milky way satellites. The $\chi^0\bar{\chi}^0 \rightarrow W^+W^-$ annihilation cross section contributed from Fig. 1 for case I is calculated to be

$$\begin{aligned}
 (\sigma_{\text{ann}}v)_{\chi\bar{\chi}} = & [I(I+1)]^2 \frac{g^4 \sqrt{s-4m_W^2}}{32\pi s^{3/2} (s-2m_W^2)} \left\{ \frac{(2m_W^2-s)(sm_\chi^2+4m_\chi^4+2m_W^4)}{(m_\chi^2(s-4m_W^2)+m_W^4)} \right. \\
 & \left. + \frac{(4m_\chi^2(s-2m_W^2)-8m_\chi^4+4m_W^4+s^2)}{\sqrt{(s-4m_\chi^2)(s-4m_W^2)}} \log \left[-\frac{\sqrt{(s-4m_\chi^2)(s-4m_W^2)}-2m_W^2+s}{\sqrt{(s-4m_\chi^2)(s-4m_W^2)}+2m_W^2-s} \right] \right\}. \quad (12)
 \end{aligned}$$

After substituting $s = 4m_\chi^2 + m_\chi^2 v^2$ into the above equation and expanding around v^2 , one obtains:

$$\langle \sigma_{\text{ann}}v \rangle = \langle a^{+-} + b^{+-}v^2 + \mathcal{O}(v^4) \rangle, \quad (13)$$

where we have

$$\begin{aligned}
 a^{+-} & \equiv [I(I+1)]^2 \frac{g^4(m_\chi^2 - m_W^2)^{3/2}}{16\pi m_\chi(2m_\chi^2 - m_W^2)^2}, \\
 b^{+-} & \equiv [I(I+1)]^2 \frac{g^4(m_\chi^2 - m_W^2)^{1/2} (24m_\chi^6 + 28m_\chi^4 m_W^2 - 36m_\chi^2 m_W^4 + 17m_W^6)}{384\pi m_\chi (2m_\chi^2 - m_W^2)^4}, \quad (14)
 \end{aligned}$$

with $g = e/\sin\theta_W$ and factor 1/2 arisen from the Dirac DM are included. We find that neglecting v^4 and higher order terms is a good approximation. In fact, substituting $v^2 = \langle v^2 \rangle$ into σv almost gives identical results to the above approximated results. For thermal relic abundance, we have $\langle v^2 \rangle = 6x_f^{-1}$ from Eq. (10), and, consequently,

$$\langle \sigma_{\text{ann}}v \rangle \simeq a^{+-} + 6\frac{b^{+-}}{x_f}, \quad J(x_f) \simeq \frac{a^{+-} + 3b^{+-}/x_f}{x_f}. \quad (15)$$

Note that for $\langle \sigma_{\text{ann}}v \rangle$ of indirect processes from milky way satellites, we have the thermal average quantity $\langle v_{1,2}^2 \rangle = v_0^2/2$, where v_0 is chosen to be the canonical value $270\sqrt{2}$ km/s [26].

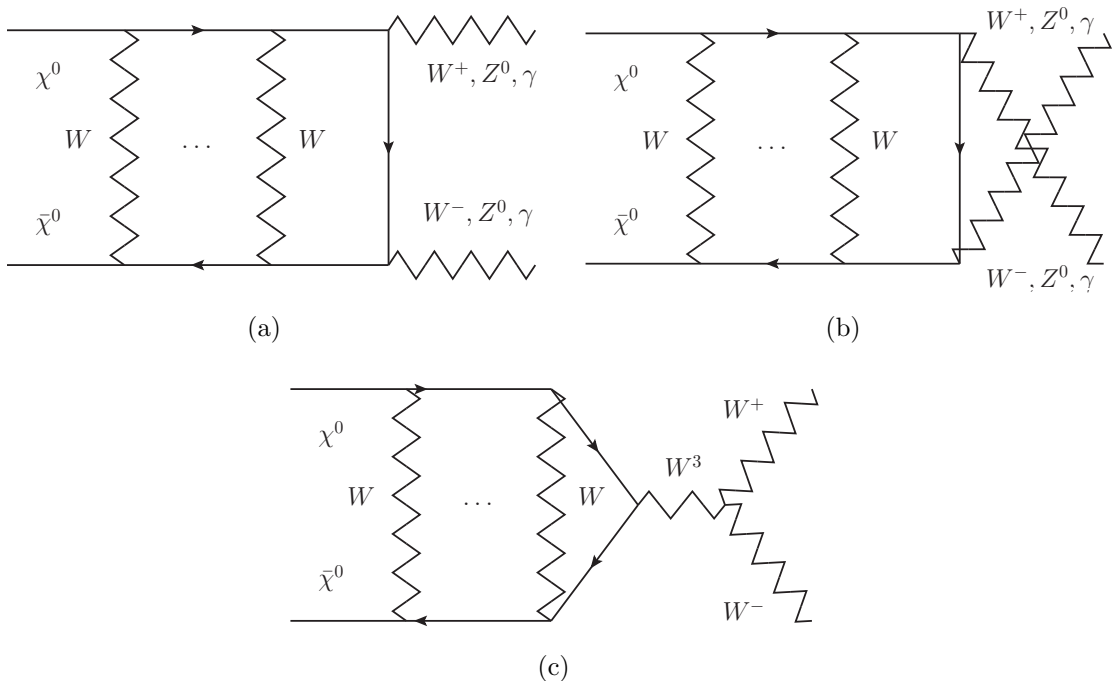


FIG. 2: (a) to (c): $\chi^0\bar{\chi}^0 \rightarrow VV$ annihilation diagrams with the Sommerfeld effect.

It is known that we need to take into account Sommerfeld enhancement effect, when the velocity is very small [27].³ In the elastic scattering case, the cross-section receives Sommerfeld enhancement as

$$\sigma v = (\sigma v)_0 S, \quad (16)$$

where $(\sigma v)_0$ corresponds to the perturbative result and S is the Sommerfeld enhancement factor. Equivalently, the amplitude receives a $S^{1/2}$ factor. For a force carrier with mass m_ϕ and couplings α , the Sommerfeld factor is given by [29]

$$S(\alpha) = \frac{\pi}{\epsilon_v} \frac{\sinh\left(\frac{2\pi\epsilon_v}{\pi^2\epsilon_\phi/6}\right)}{\cosh\left(\frac{2\pi\epsilon_v}{\pi^2\epsilon_\phi/6}\right) - \cos\left(2\pi\sqrt{\frac{1}{\pi^2\epsilon_\phi/6} - \frac{\epsilon_v^2}{(\pi^2\epsilon_\phi/6)^2}}\right)}, \quad (17)$$

with

$$\epsilon_v \equiv \frac{v}{\alpha}, \quad \epsilon_\phi \equiv \frac{m_\phi}{\alpha m_\chi}. \quad (18)$$

Note that we have $S > 1$ for $\alpha > 0$ and vice verse.

The Sommerfeld enhancement in the present case is rather involved, since the $\chi^0\bar{\chi}^0$ state can rescatter into other states, such as $\chi^\pm\bar{\chi}^\pm$ and so on, through t -channel diagrams by exchanging W and Z with the rescattered state annihilated into W^+W^- (see Fig. 2). To simplify the calculation we follow [24, 30] to consider the SU(2) symmetric limit. For a generic isospin I , scatterings

³ Some authors[13] also called this as Sakharov effect [28].

$\chi^j \overline{\chi^j} \rightarrow \chi^i \overline{\chi^i}$ (with $i, j = -I, -I+1, \dots, I-1, I$) produce a potential $V_{ij} = -|V_W| \sum_{c=1,2,3} T_{ij}^c T_{ji}^c$ with $|V_W| = \alpha_W e^{-m_W z r} / r$.⁴

To proceed we use a procedure that is similar to those used in the study of final state interaction [31]. We note that the potential can be diagonalized into several irreducible representations:⁵

$$V_{ij} = \sum_{L=1}^{2I} (U^T)_{iL} \{-[I(I+1) - L(L+1)/2] |V_W|\} U_{Lj}, \quad (19)$$

with

$$U_{Lj} = (-1)^j \langle IjI(-j) | L0 \rangle, \quad (20)$$

where $\langle IjI(-j) | L0 \rangle$ is the ClebschGordan coefficient (in the $\langle j_1 m_1 j_2 m_2 | JM \rangle$ notation). The irreducible parts of V do not mixed in further rescattering as it is easy to see that $(V^n)_{ij} = \sum_L U_{iL}^T \{-[I(I+1) - L(L+1)/2] |V_W|\}^n U_{Lj}$. The Sommerfeld enhancement factor of the irreducible parts can be obtained as the elastic case and, consequently, we have

$$\mathcal{S}_{ij} = \sum_{L=1}^{2I} U_{iL}^T S([I(I+1) - L(L+1)/2] \alpha_W) U_{Lj}, \quad (21)$$

where $S(\alpha)$ is given by Eq. (17) but with $m_\phi = m_{W,Z}$. The $\chi^0 \overline{\chi^0} \rightarrow W^+ W^-$ amplitude with Sommerfeld enhancement, A_S , is now given by

$$A_S(\chi^0 \overline{\chi^0} \rightarrow W^+ W^-) = \sum_i A(\chi^i \overline{\chi^i} \rightarrow W^+ W^-) \mathcal{S}_{i0}^{1/2}, \quad (22)$$

where i is summed over all $\chi^i \overline{\chi^i}$ states. Therefore, the Sommerfeld enhanced s -wave part of σv is given by

$$a_S^{+-} = \sum_{i,j} \mathcal{S}_{0i}^{1/2} a_{ij}^{+-} \mathcal{S}_{j0}^{1/2}, \quad (23)$$

where i and j are summed over $\chi^i \overline{\chi^i}$ and $\chi^j \overline{\chi^j}$ states, respectively, and a_{ij}^{+-} corresponds to the contribution from the $A^*(\chi^i \overline{\chi^i} \rightarrow W^+ W^-) A(\chi^j \overline{\chi^j} \rightarrow W^+ W^-)$ part.

It is straightforward to obtain

$$a_{ij}^{+-} = \frac{g^4 (m_\chi^2 - m_W^2)^{3/2}}{32\pi m_\chi (4m_\chi^2 - m_W^2)^2 (2m_\chi^2 - m_W^2)^2} \{2[I(I+1) - i^2][I(I+1) - j^2] (4m_\chi^2 - m_W^2)^2 + ij(4m_\chi^3 + 20m_\chi^2 m_W^2 + 3m_W^4)\} \quad (24)$$

with factor 1/2 included, and, consequently,

$$a_S^{+-} = a^{+-} \frac{1}{9} \left[2S^{1/2}(I(I+1)\alpha_W) + S^{1/2}([-3 + I(I+1)]\alpha_W) \right]^2. \quad (25)$$

⁴ Note that we differ from [24, 30] as we do not consider $\overline{\chi^i}$ to be identical to χ^{-i} . Therefore we do not have the factor of $\sqrt{2}$ on the $\chi^0 \overline{\chi^0}$ state (for i or $j = 0$) from the identical particle effect and we have a V matrix with larger dimension.

⁵ The expression is obtained with the help of $\sum_c T_{ij}^c T_{ji}^c = -\sum_c T_{ij}^c T_{-i-j}^c (-)^{i-j}$ and the standard method of addition of angular momentum.

Note that a similar expression holds for the Sommerfeld enhanced b term (b_S). Finally, we obtain

$$\langle \sigma^{+-} v \rangle = \left\langle (\sigma^{+-} v)_0 \frac{1}{9} \left[2S^{1/2}(I(I+1)\alpha_W) + S^{1/2}([-3 + I(I+1)]\alpha_W) \right]^2 \right\rangle. \quad (26)$$

In the $S \rightarrow 1$ limit $\langle \sigma^{+-} v \rangle$ reduces to the one given in Eq. (13). Furthermore, if the eigenvalues of V_{ij} were degenerate, we return to the elastic result as in Eq. (16).

Note that through rescattering we can also have $\chi^0 \bar{\chi}^0 \rightarrow Z^0 Z^0, Z^0 \gamma, \gamma \gamma$ annihilations, with

$$\begin{aligned} A_S(\chi^0 \bar{\chi}^0 \rightarrow Z^0 Z^0) &= \sum_i A(\chi^i \bar{\chi}^i \rightarrow Z^0 Z^0) \mathcal{S}_{i0}^{1/2} \\ A_S(\chi^0 \bar{\chi}^0 \rightarrow Z^0 \gamma) &= \sum_i A(\chi^i \bar{\chi}^i \rightarrow Z^0 \gamma) \mathcal{S}_{i0}^{1/2}, \\ A_S(\chi^0 \bar{\chi}^0 \rightarrow \gamma \gamma) &= \sum_i A(\chi^i \bar{\chi}^i \rightarrow \gamma \gamma) \mathcal{S}_{i0}^{1/2}, \end{aligned} \quad (27)$$

and, consequently,

$$a_S^{00,0\gamma,\gamma\gamma} = \sum_{i,j} \mathcal{S}_{0i}^{1/2} a_{ij}^{00,0\gamma,\gamma\gamma} \mathcal{S}_{j0}^{1/2}, \quad (28)$$

with

$$a_{ij}^{00} = \frac{g^4 \cos^4 \theta_W (m_\chi^2 - m_Z^2)^{3/2} i^2 j^2}{8\pi m_\chi (2m_\chi^2 - m_Z^2)^2}, \quad a_{ij}^{0\gamma} = \frac{e^2 g^2 \cos^2 \theta_W (4m_\chi^2 - m_Z^2) i^2 j^2}{64\pi m_\chi^4}, \quad a_{ij}^{\gamma\gamma} = \frac{e^4 i^2 j^2}{32\pi m_\chi^2}, \quad (29)$$

and similar expressions for b terms. These processes also contribute to the relic density and are the inevitable consequences and signatures of inelastic Sommerfeld effects.

We obtain the annihilation cross sections for $\chi^0 \bar{\chi}^0 \rightarrow Z^0 Z^0, Z^0 \gamma, \gamma \gamma$ as

$$\langle \sigma^\alpha v \rangle = \left\langle (a^\alpha + b^\alpha v^2) \frac{1}{9} \left[S^{1/2}(I(I+1)\alpha_W) - S^{1/2}([-3 + I(I+1)]\alpha_W) \right]^2 \right\rangle, \quad (30)$$

with $\alpha = 00, 0\gamma, \gamma\gamma$ and

$$\begin{aligned} (a^{00}, b^{00}) &= 2(a^{+-}, b^{+-})|_{g \rightarrow g \cos \theta_W, m_W \rightarrow m_Z}, \\ (a^{\gamma\gamma}, b^{\gamma\gamma}) &= 2(a^{+-}, b^{+-})|_{g \rightarrow e, m_W \rightarrow 0}, \\ a^{0\gamma} &= [I(I+1)]^2 \frac{e^2 g^2 \cos^2 \theta_W (4m_\chi^2 - m_Z^2)}{64\pi m_\chi^4}, \\ b^{0\gamma} &= [I(I+1)]^2 e^2 g^2 \cos^2 \theta \frac{12m_\chi^4 + 13m_\chi^2 m_Z^2 - m_Z^4}{192\pi m_\chi^4 (4m_\chi^2 - m_Z^2)}, \end{aligned} \quad (31)$$

where factor 1/2 are included. It is clear that these $\langle \sigma^\alpha v \rangle$ s go to zero in the $S \rightarrow 1$ or in the degenerate limit. Note that we do not include loop contribution in these modes, since in most cases the contributions from inelastic rescattering parts are larger than the perturbative ones. We are ready to perform numerical study, where results will be given in the next section.

II. $\mathbf{I = Y = 0}$ case

In this case, the DM candidate is a pure weak isospin singlet Dirac fermion. The case that DM is a scalar has been discussed by others [5, 7]. To reproduce the observed relic density, we need to

couple χ to SM fermions f . We consider renormalizable interaction only. Therefore, an additional particle X is necessary to mediate the $\chi\bar{\chi} \rightarrow f\bar{f}$ annihilation process. Since the DM is a weak isospin singlet, the mediator can only be a singlet and the $\bar{f}f$ bilinear term that couple to X should be a singlet as well. It is easy to see that the $\bar{f}f$ bilinear term can only take the forms of $\bar{f}_L\gamma_\mu f_L$ and $\bar{f}_R\gamma_\mu f_R$, and hence the mediator particle X should be a vector boson, if only renormalizable interaction is allowed.⁶

The Lagrangian involving χ , f and X is given by:

$$\begin{aligned} \mathcal{L} = & \mathcal{L}_{\text{SM}} + \bar{\chi} \left(i\mathcal{D}^{(\chi)} - m_\chi \right) \chi + \sum_f \left(\bar{f}_L i\mathcal{D}^{(L)} f_L + \bar{f}_R i\mathcal{D}^{(R)} f_R - \lambda_f \bar{f}_L H f_R - \lambda_f \bar{f}_R H^\dagger f_L \right) \\ & - \frac{1}{4} \mathcal{X}^{\mu\nu} \mathcal{X}_{\mu\nu} + \frac{1}{2} M_X^2 X^\mu X_\mu. \end{aligned} \quad (32)$$

with

$$D_\mu^{(\chi)} \chi = (\partial_\mu + i g_\chi X_\mu) \chi, \quad D_\mu^{(L,R)} f_{(L,R)} = \left(\partial_\mu + i g_f^{(L,R)} X_\mu \right) f_{(L,R)} \quad (33)$$

and $\mathcal{X}_{\mu\nu} = \partial_\mu X_\nu - \partial_\nu X_\mu$ and the SM fermions f s pick up masses from Higgs mechanism (using the Higgs doublet H) as usual. Here g_χ , $g_f^{(L,R)}$ are corresponding coupling constants and $f_{(L,R)}$ is left (right) fermion. For simplicity, we only consider a vector-type interaction, $g_f^L = g_f^R$. The interaction term of the Lagrangian can be recast as:

$$\mathcal{L}_{\text{int}} = -g_\chi \bar{\chi} \gamma^\mu \chi X_\mu - \sum_f g_f^V \bar{f} \gamma^\mu f X_\mu \quad (34)$$

with $g_f^V = \frac{1}{2}(g_f^L + g_f^R)$. In order to determine the relic density of DM particles, we need to calculate the cross section of DM annihilation to fermion pairs. The result is given by

$$(\sigma_{\text{ann}})_{\chi\bar{\chi}} = \frac{M_X}{\sqrt{s}} \times \frac{g_\chi^2}{(s - M_X^2)^2 + M_X^2 \Gamma_{\text{tot}}^2} \frac{\sum_f \Gamma(\tilde{X} \rightarrow \bar{f}f)}{\sqrt{s - 4m_\chi^2}} (s + 2m_\chi^2), \quad (35)$$

with

$$\Gamma(\tilde{X} \rightarrow \bar{f}f) \equiv \frac{N_f^c g_f^{V2} \sqrt{M_{\tilde{X}}^2 - 4m_f^2}}{12\pi M_{\tilde{X}}^2} (M_{\tilde{X}}^2 + 2m_f^2), \quad (36)$$

where $s = 2m_\chi^2(1 + 1/\sqrt{1 - v^2})$ is the square of the center-of-mass energy; $\Gamma(\tilde{X} \rightarrow \bar{f}f)$ is the decay width of ‘‘virtual’’ X with mass $M_{\tilde{X}} = \sqrt{s}$ and N_f^c is the number of color of the f -fermion.

We have to calculate $\langle \sigma_{\text{ann}} v \rangle$ numerically, since the standard method (Taylor expand) gives extremely poor results near the pole, even producing negative cross section [33].⁷ We can determine the validity parameter space of g_χ and g_f^V using the constraint from thermal relic abundance and direct detection for any given values of m_χ , M_X . Note that in this case, the Sommerfeld enhancement is irrelevant. As we shall see, we need to make use of the resonant effect to give viable results on relic density without violating the direct search data. In that region ($m_\chi \sim m_X/2$), the Sommerfeld factor S as given by Eq. (17) is very close to unity.

⁶ We are different from [32] in this respect, where they have scalar mediator.

⁷ It is noted that the original integrated upper limit is infinity (see Eq.(10)). Here we modified it to 1, because the relative velocity v cannot be larger than light speed.

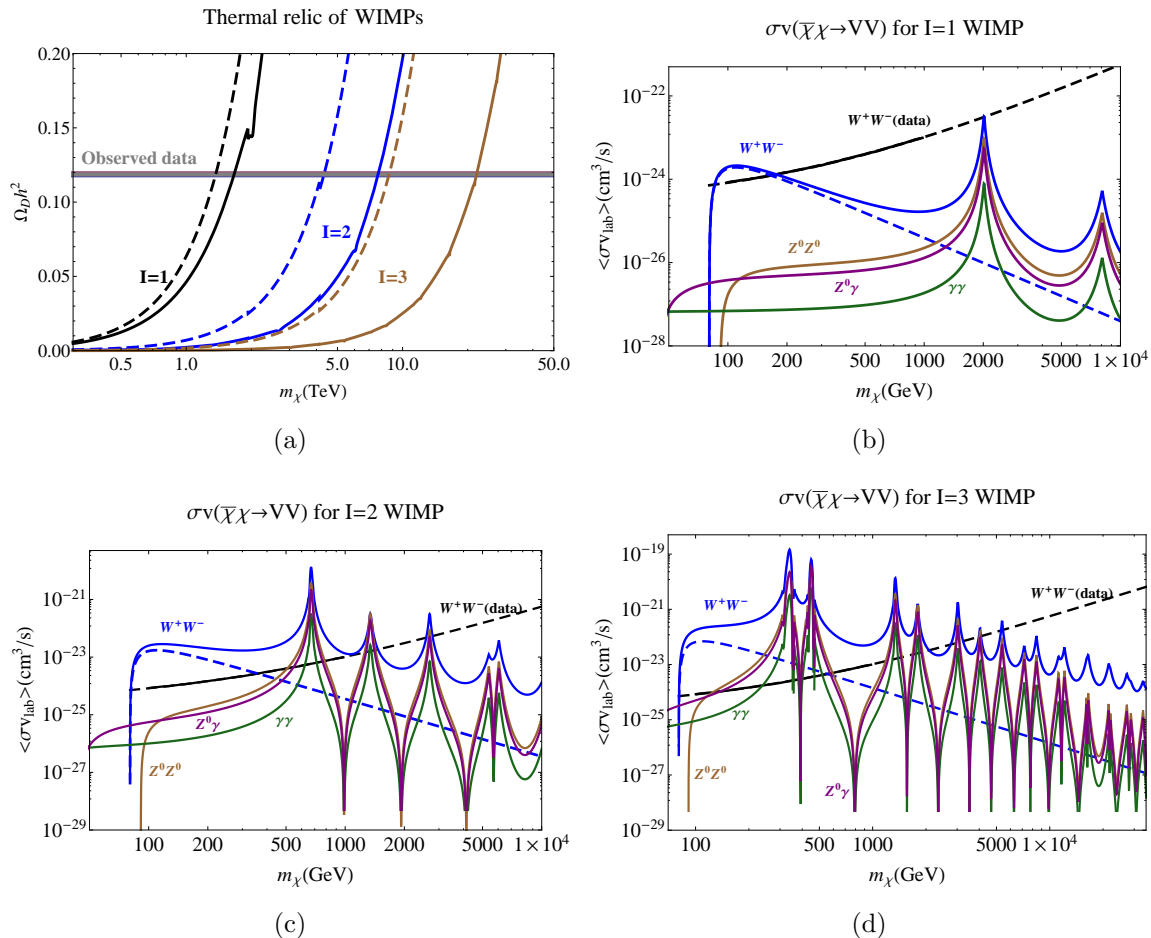


FIG. 3: (a) Predicted relic density fractions for $I = 1, 2, 3$ compared to the data, $\Omega_{\text{nbm}} h^2 = 0.1187 \pm 0.0017$ [2]. The solid (dashed) lines are with (without) the Sommerfeld factor. (b) to (d): The galactic DM annihilation cross sections for W^+W^- , Z^0Z^0 , $Z^0\gamma$, $\gamma\gamma$ channels for different $I = 1, 2, 3$ cases. The solid (dashed) lines are the results with (without) the Sommerfeld factor. The W^+W^- data is from [25] with both ends extrapolated.

III. NUMERICAL RESULTS

I. $\mathbf{I} \neq 0, \mathbf{I}_3 = \mathbf{Y} = 0$ case

We first give the results of case I. In Fig. 3(a) we show our results on relic abundance for $I = 1, 2, 3$ and compare to the experimental result $\Omega_{\text{nbm}} h^2 = 0.1187 \pm 0.0017$ [2]. We take $x_f \simeq 24$ to simplify the calculations. Solid (dashed) lines are results with (without) the Sommerfeld factor. We see that the observed relic density can be reproduced in all three cases with TeV DM masses (see also the third column of Table I). Without the Sommerfeld factor, the masses scale as $I(I+1)$. The Sommerfeld enhancement become more prominent in the large I case, and, consequently, the mass grows faster than the simple scaling. From the figure one may easily infer that the DM masses to give correct DM relic density are larger than 50 TeV for $I > 4$ and, hence, for practical purpose

TABLE I: m_χ lower limits (m_χ^{LL}) obtained from Fermi-Lat constraints on $\chi\bar{\chi} \rightarrow W^+W^-$ rates, m_χ required to give correct thermal relic and the Galactic $\langle\sigma v\rangle$ at the corresponding dark matter masses are shown. Dark matter masses are shown in TeV, while $\langle\sigma v\rangle$ in cm^3/s . Values in parenthesis are obtained without using the Sommerfeld enhancement factors.

Isospin	m_χ^{LL} (Indirect)	m_χ (Relic)	$\langle\sigma v\rangle(W^+W^-)$	$\langle\sigma v\rangle(Z^0Z^0)$	$\langle\sigma v\rangle(Z^0\gamma)$	$\langle\sigma v\rangle(\gamma\gamma)$
$I = 1$	0.176(0.166)	$1.67 \pm 0.01(1.37 \pm 0.01)$	1.3×10^{-24}	3.3×10^{-25}	1.9×10^{-25}	2.7×10^{-26}
$I = 2$	1.468 ^a (0.359)	$7.72 \pm 0.05(4.33 \pm 0.03)$	1.2×10^{-24}	1.8×10^{-26}	1.0×10^{-26}	1.5×10^{-27}
$I = 3$	5.446 ^a (0.556)	$21.93_{-0.08}^{+0.19}(8.67 \pm 0.06)$	1.5×10^{-23}	2.6×10^{-25}	1.5×10^{-25}	2.2×10^{-26}

^aInferred by comparing to the extrapolated Femi-LAT data.

we shall restrict I up to 3.

In Fig. 3(b) to (d) we show the results of galactic $\langle\sigma v\rangle$ on WIMP annihilation for $\chi^0\bar{\chi}^0 \rightarrow W^+W^-, Z^0Z^0, Z^0\gamma, \gamma\gamma$ channels for WIMP candidates with different isospin ($I = 1, 2, 3$) and compare them to the milky way satellites data on the W^+W^- rate [25]. We see that, when the Sommerfeld factor are removed, the W^+W^- data constraints the DM masses to be heavier than few hundred GeV. However, except for $I = 1$, all DM with sub-TeV mass are excluded when the Sommerfeld enhancements are included (see also the second column of Table I). The signatures of the enhancement are sizable $Z^0Z^0, Z^0\gamma, \gamma\gamma$ rates. It will be interesting to search for these processes.

In Table I results on m_χ lower limits (m_χ^{LL}) obtained from Fermi-Lat constraints on $\chi\bar{\chi} \rightarrow W^+W^-$ rates, m_χ required to give correct thermal relic and the Galactic $\langle\sigma v\rangle$ at the corresponding dark matter masses are collected. Note that these $\langle\sigma v\rangle$ are different from and, in fact, much than their counter part in the $x_f = 24$ period as the Sommerfeld factors are more effective here. Note that our results on $I = 2$ are similar to those in [18, 24].

In this case we do not consider direct search as there is no data on the interesting mass regions to give the correct relic density in present and near future experiments.

II. $\mathbf{I} = \mathbf{0}, \mathbf{I}_3 = \mathbf{Y} = \mathbf{0}$ case

We now turn to case II. We shall discuss the valid parameter space first. To simplify the numerical analysis, instead of solving Eq. (8) directly, we set the parameter value $x_f = 24$, which is checked to be a good approximation, and assume the coupling constant g_f^V to be proportional to g_χ with $n \equiv g_f^V/g_\chi$. The proportionality of couplings may come from some underlying gauge symmetries, which we will not go further into.

For given values of mediator mass M_X and coupling ratio n , we can solve g_χ numerically by substituting Eq.(35) into Eq.(7) and (9). The results are shown in Fig. 4. In Fig. 4(a)-(c), we show the allowable range for the parameter g_χ as a function of the DM mass with $\Omega_{\text{nbm}}h^2 = 0.1187 \pm 0.0017$ for different mediator mass, namely $M_X = 1000, 800$ and 600 GeV. In each figure, the curve from top to bottom, we adopt $n = 0.1, 1$ and 2 . The shaded region are the allowed region of g_χ (with increasing n from top to bottom), which constrained by the Xenon100 results [34] of the spin-independent DM-nucleon elastic scattering process. We note that the g_χ curve was bent down

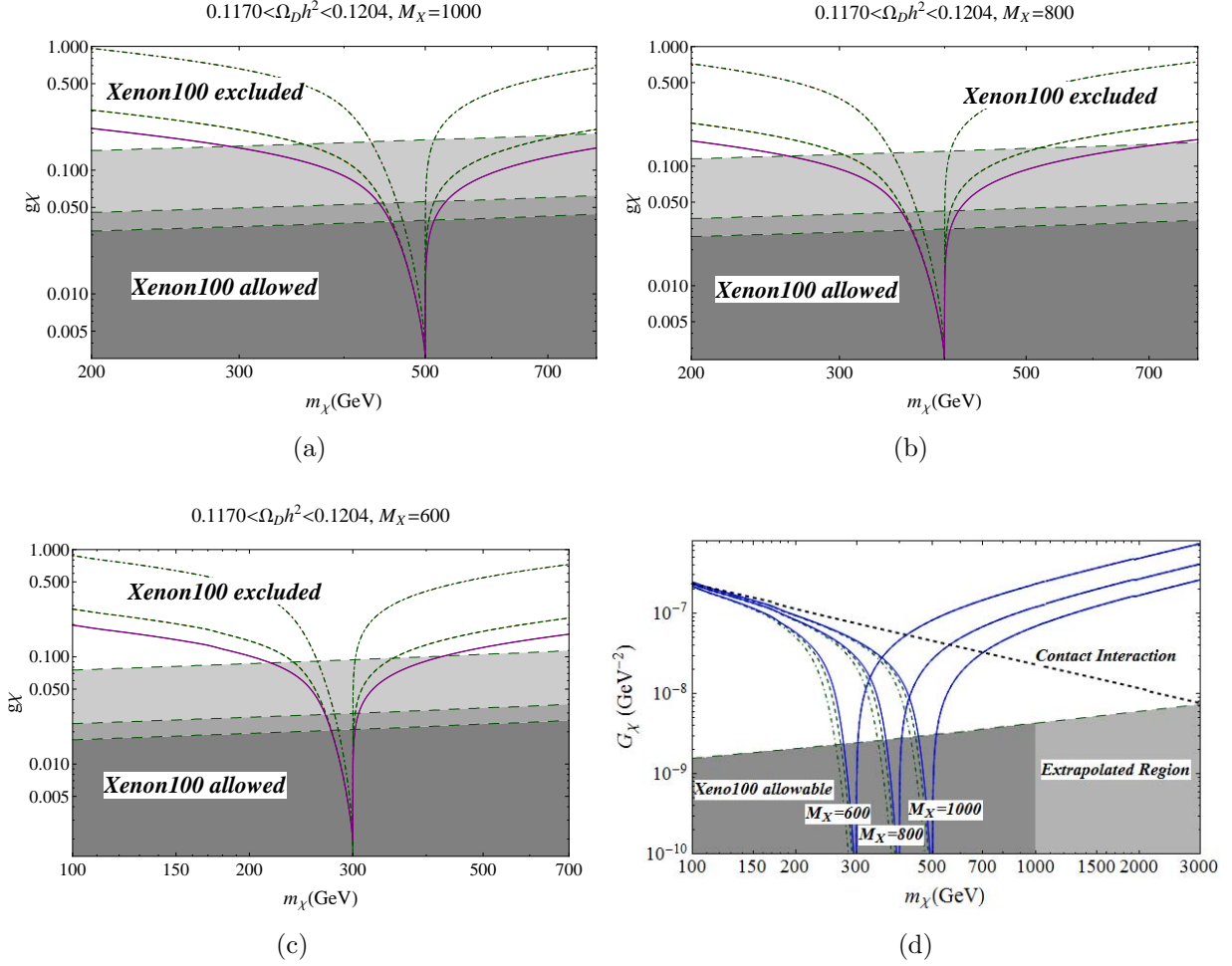


FIG. 4: (a)-(c) The g_χ function for $M_X = 1000, 800$ and 600 GeV separately. In each figure, from top to bottom, we adopt $g_f^V = 0.1g_\chi$, g_χ and $2g_\chi$ to show the allowed range with $\Omega_{\text{nbm}}h^2 = 0.1187 \pm 0.0017$. The shadow region, from top to bottom, also corresponding to g_χ constrained by Xenon100 experiment [34] for different n . (d) Combining (a)-(c) results using the coupling constant G_χ . The black (short dashed) line is corresponding to contact interaction. The blue (solid) and green (dot-dashed) lines are for containing BW resonance effect. The light gray shadow region was obtained by extrapolating the Xenon100's result.

to Xenon100 allowable region around resonance point. It is this Breit-Wigner (BW) resonance effect that make the model to survive from the Xenon100 experimental bound.

To further explore the physical meaning, we define a new coupling constant G_χ such as

$$G_\chi \equiv \frac{g_\chi g_f^V}{M_X^2}. \quad (37)$$

In Fig. 4(d), we combing results in Fig. 4(a)-(d) using G_χ . We also plot the G_χ of the contact interaction case, where the resonance effect is neglected and consider only (the first term of) the contact interaction,

$$\mathcal{L}_{\text{eff}} = -G_\chi \sum_f [\bar{\chi}\gamma^\mu\chi\bar{f}\gamma_\mu f + n\bar{f}\gamma^\mu f\bar{f}\gamma_\mu f], \quad (38)$$

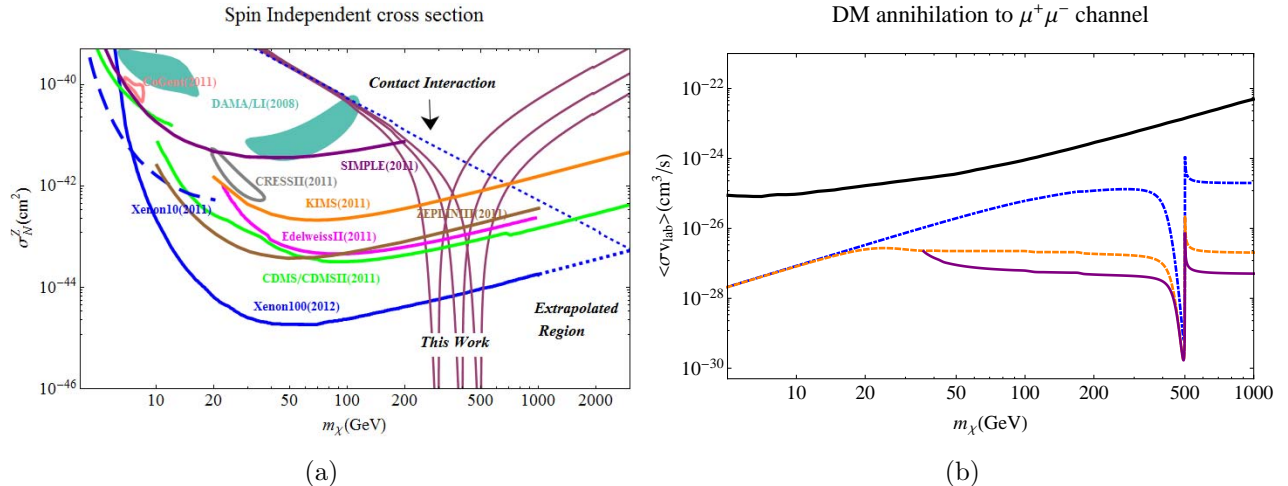


FIG. 5: (a) The magnitude of elastic scattering cross section of our model for $M_X = 600, 800, 1000$ GeV with $n = 1$ and direct detection results which obtained from different experimental group [20]. We see that the BW effect indeed affect the behavior of the curve in the resonant region. The result of contact interaction also be showed. It reveals that the contact interaction model can only survive at large DM mass region ($m_\chi \gtrsim 3$ TeV). (b) The DM annihilation cross section of indirect search for the $\mu^+\mu^-$ channel. The blue(dot-dashed), orange(dashed) and purple(solid) curve are corresponding to $g_f^V = 0.1g_\chi, g_\chi$ and $2g_\chi$ separately with $M_X = 1000$ GeV and are compared to the black solid line corresponding to the FermiLAT result [25].

which can be obtained from Eq. (32) by integrating out the mediator particle X when $m_X \gg m_\chi$. It is shown in [35] that for an effective eq contact interaction operator $\eta_{VV}^{eq}(\bar{e}\gamma_\mu e)(\bar{q}\gamma^\mu q)$, the effective coupling constant η_{VV}^{eq} (which is equal to nG_χ in our model) has an upper limit with $nG_\chi = \eta_{VV}^{eq} \lesssim 5.01 \times 10^{-8}$. This bound is comparable to the Xenon100 bound limit $G_\chi \lesssim 3 \times 10^{-9}$ (see Fig. 4(d)).

We see that, as expected, for $m_\chi \ll M_X/2$ the results (of renormalizable interactions) are similar to the one from the contact interaction, while for $m_\chi \gtrsim M_X/2$, the curves are different, since s is no longer less than m_X^2 (see Eq. (35)). The curve from the contact interaction can only satisfy the projected (extrapolated) Xenon100 bound for $m_\chi \gtrsim 3$ TeV. In other words, the model is ruled out for $m_\chi \lesssim 3$ TeV, if the BW effect is absent. However, with the present of the BW effect, the model can survive from the direct search bound with m_χ even as low as few hundreds GeV. Furthermore, the allowable windows of m_χ become broader for smaller n (see Fig. 4(d)). For example, for $m_X = 1000$ GeV with $n = 2, 1$ and 0.1 , dark matters having $m_\chi = 500_{-45.89}^{+12.75}$, $500_{-54.58}^{+12.75}$ and $500_{-69.38}^{+12.75}$ GeV, respectively, can evade the direct search bound.

The corresponding typically elastic cross section σ_N^Z for DM and nuclei is normalized to DM-proton elastic cross section σ_p such that (see Appendix A)

$$\sigma_N^Z = \sigma_p = \frac{9\mu_p^2}{\pi} G_\chi^2 \quad (39)$$

with reduced mass $\mu_p = m_\chi m_p / (m_\chi + m_p)$. The result is shown in Fig. 5(a). In the figure we demonstrate the elastic scattering cross section curves of our model for $M_X = 600, 800, 1000$ GeV

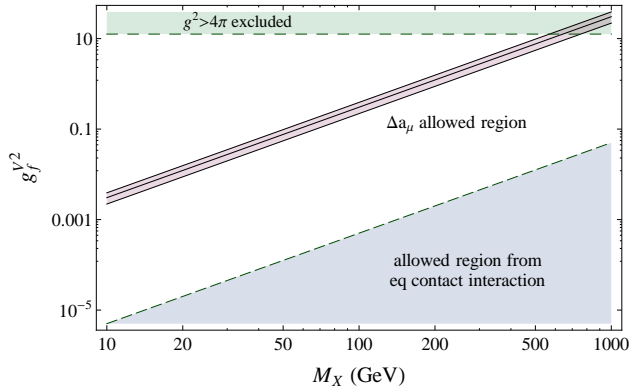


FIG. 6: The band corresponds to the expected parameter space to saturate Δa_μ . The shaded region in the lower right corner is the allowed region from eq contact interaction.

with $n = 1$ and the contact interaction model. As mentioned with the resonance effect, the model can survive from the direct search bound.

In addition to the direct search result, we also calculate the DM annihilation cross section of indirect search for the $\mu^+\mu^-$ channel. The result is showed in Fig. 5(b). The blue(dot-dashed), orange(dashed) and purple(solid) curves are corresponding to $M_X = 1000$ GeV with $g_f^V = 0.1g_\chi$, g_χ and $2g_\chi$, respectively.

IV. DISCUSSION AND CONCLUSIONS

The muon $g - 2$ puzzle could be a hint for some unknown contributions from physics beyond the SM. It will be interesting to explore the connection with the DM sector. In Fig. 6, we show the expected parameter space to saturate Δa_μ [3]. Since the expected parameter space in case II is excluded by $(g_f^V/M_X)^2 = \eta_{VV}^{eq} \lesssim 5.01 \times 10^{-8}$ [35], we conclude that our model is not sufficient to explain the deviation.

It is important to experimentally distinguish case I and case II. We note that case I has sizable Sommerfeld enhancement in $\chi^0\bar{\chi}^0 \rightarrow W^+W^-, Z^0Z^0, Z^0\gamma, \gamma\gamma$ rates, which are relevant to indirect searches. For example, the W^+W^- rate is enhanced by two order of magnitude from the canonical annihilation rate reaching 10^{-24} cm^3s^{-1} (see Table I). Fermi-LAT and iceCube will be able to search for these signatures in the future. On the other hand the indirect searches on the case II part is more or less standard. We do not expect rates to differ much from the canonical one. For example in Fig. 5(b), we see that the $\mu^+\mu^-$ rate is roughly 10^{-26} cm^3s^{-1} , as the Sommerfeld enhancement in this case is negligible.

In conclusion, we study pure weak eigenstate Dirac fermionic dark matters. We consider WIMP with renormalizable interaction. According to results of direct searches and the nature of DM, the quantum number of DM is determined to be $I_3 = Y = 0$. There are only two possible cases: either DM has non-vanishing weak isospin ($I \neq 0$) or it is an isosinglet ($I = 0$). In the first case, we find that the Sommerfeld enhancement is sizable for large I DM, producing large $\chi^0\bar{\chi}^0 \rightarrow W^+W^-, Z^0Z^0, Z^0\gamma, \gamma\gamma$ rates. In particular, we obtain large $\chi\bar{\chi} \rightarrow W^+W^-$ cross section,

which is comparable to the latest bounds from indirect searches and m_χ is constrained to be larger than few hundred GeV to few TeV. It is possible to give correct relic density with m_χ higher than these lower bounds. In the second case, to couple DM to standard model particles, a SM-singlet vector mediator X is required from renormalizability and SM gauge quantum numbers. To satisfy the latest bounds of direct searches and to reproduce the DM relic density at the same time, resonant enhancement in DM annihilation diagram is needed. Thus, the masses of DM and the mediator are related. Our model is not sufficient to explain the Δa_μ deviation.

Acknowledgments

We thanks Yi-Chin Yeh and Ho-Chin Tsai for discussions. This research was supported in part by the National Center for Theoretical Sciences and the National Science Council of R.O.C. under grant No NSC100-2112-M-033-001-MY3 and NSC101-2811-M-033-016.

=====

Appendix A: DM-nucleon elastic cross section

In this appendix, to avoid confusion, we will give some definitions to different DM scattering cross section. The first is DM-nucleus zero momentum transfer spin-independent(SI) cross section,

$$\sigma_A^{\text{SI}} = \frac{m_\chi^2 m_A^2}{\pi(m_\chi + m_A)^2} \times \frac{g_\chi^2}{M_X^4} [f_p Z + f_n (A - Z)]^2 \quad (\text{A1})$$

where m_A is the mass of target nucleus with Z protons and $A - Z$ neutrons and $f_{p,n}$ are the couplings to protons and neutrons with $f_{p,n} = 2g_{u,d}^V + g_{d,u}^V = 3g_f^V$ in this model. By above equation, for $Z = A = 1$, we then have DM-proton cross section $\sigma_p = 9\mu_p^2 (g_\chi g_f^V)^2 / (\pi M_X^4) = 9\mu_p^2 G_\chi^2 / \pi$. The third is total cross section $\sigma_t = \sum_i \eta_i \sigma_{A_i}$. Here the summation is over isotopes A_i with fractional number abundance η_i since it is usually to include the possibility of multiple isotopes for each detector in laboratory. To conciliate results from different detectors, one usually normalize the total cross section to one nucleon cross section σ_N^Z such as

$$\sigma_N^Z = \sigma_t / N = \frac{\sigma_p}{N \mu_p^2} \sum_i \eta_i \mu_{A_i}^2 [Z + (A_i - Z) f_n / f_p]^2. \quad (\text{A2})$$

with N is normalization constant. For $f_p / f_n = 1$ (isospin symmetry), it is easy to obtain $\sigma_N^Z = \sigma_p \sum_i \eta_i (\mu_{A_i} A_i / \mu_p)^2 / N$. Because for one isotope dominated detector, say, with proton as target, the normalized cross section should be equal to DM-proton cross section. We then have $N = \sum_i \eta_i (\mu_{A_i} A_i / \mu_p)^2$ and hence $\sigma_N^Z = \sigma_p$ for different detector.

[1] G. Hinshaw *et al.* [WMAP Collaboration], “Nine-Year Wilkinson Microwave Anisotropy Probe (WMAP) Observations: Cosmological Parameter Results,” arXiv:1212.5226 [astro-ph.CO].

- [2] P. A. R. Ade *et al.* [Planck Collaboration], “Planck 2013 results. I. Overview of products and scientific results,” arXiv:1303.5062 [astro-ph.CO].
- [3] J. Beringer *et al.* [Particle Data Group Collaboration], “Review of Particle Physics (RPP),” Phys. Rev. D **86**, 010001 (2012).
- [4] M. Drees and G. Gerbier, “Mini-Review of Dark Matter: 2012,” arXiv:1204.2373 [hep-ph].
- [5] J. McDonald, “Gauge singlet scalars as cold dark matter,” Phys. Rev. D **50**, 3637 (1994).
- [6] C. P. Burgess, M. Pospelov and T. ter Veldhuis, “The Minimal model of nonbaryonic dark matter: A Singlet scalar,” Nucl. Phys. B **619**, 709 (2001) [hep-ph/0011335].
- [7] X.G. He, T. Li, X.Q. Li, J. Tandean and H.C. Tsai, “Constraints on Scalar Dark Matter from Direct Experimental Searches,” Phys. Rev. D **79**, 023521 (2009).
- [8] M. Gonderinger, Y. Li, H. Patel and M. J. Ramsey-Musolf, “Vacuum Stability, Perturbativity, and Scalar Singlet Dark Matter,” JHEP **1001**, 053 (2010) [arXiv:0910.3167 [hep-ph]].
- [9] A. Drozd, B. Grzadkowski and J. Wudka, “Multi-Scalar-Singlet Extension of the Standard Model - the Case for Dark Matter and an Invisible Higgs Boson,” JHEP **1204**, 006 (2012) [arXiv:1112.2582 [hep-ph]].
- [10] K. Cheung, Y. -L. S. Tsai, P. -Y. Tseng, T. -C. Yuan and A. Zee, “Global Study of the Simplest Scalar Phantom Dark Matter Model,” JCAP **1210**, 042 (2012) [arXiv:1207.4930 [hep-ph]].
- [11] N. Okada and T. Yamada, “Simple fermionic dark matter models and Higgs boson couplings” arXiv:1304.2962 [hep-ph].
- [12] Y. .B. Zeldovich, A. A. Klypin, M. Y. .Khlopov and V. M. Chechetkin, “Astrophysical constraints on the mass of heavy stable neutral leptons,” Sov. J. Nucl. Phys. **31**, 664 (1980) [Yad. Fiz. **31**, 1286 (1980)].
- [13] K. Belotsky, D. Fargion, M. Khlopov and R. V. Konoplich, “May heavy neutrinos solve underground and cosmic ray puzzles?,” Phys. Atom. Nucl. **71**, 147 (2008) [hep-ph/0411093].
- [14] Y. G. Kim, K. Y. Lee and S. Shin, “Singlet fermionic dark matter,” JHEP **0805**, 100 (2008) [arXiv:0803.2932 [hep-ph]].
- [15] K. Cheung and T. -C. Yuan, “Hidden fermion as milli-charged dark matter in Stueckelberg Z- prime model,” JHEP **0703**, 120 (2007) [hep-ph/0701107].
- [16] D. Feldman, Z. Liu, P. Nath and G. Peim, “Multicomponent Dark Matter in Supersymmetric Hidden Sector Extensions” Phys. Rev. D **81**, 095017 (2010). arXiv:1004.0649 [hep-ph]
- [17] S. Andreas, M. D. Goodsell and A. Ringwald, “Dark Matter and Dark Forces from a Supersymmetric Hidden Sector,” Phys. Rev. D **87**, 025007 (2013) [arXiv:1109.2869 [hep-ph]].
- [18] M. Cirelli, N. Fornengo and A. Strumia, “Minimal dark matter,” Nucl. Phys. B **753**, 178 (2006) [hep-ph/0512090].
- [19] B. W. Lee and S. Weinberg, “Cosmological Lower Bound on Heavy Neutrino Masses,” Phys. Rev. Lett. **39**, 165 (1977).
- [20] <http://dmtools.brown.edu:8080/session/new>.
- [21] D. Hooper, “The Empirical Case For 10 GeV Dark Matter,” Phys. Dark Univ. **1**, 1 (2012) [arXiv:1201.1303 [astro-ph.CO]].
- [22] E.W. Kolb and M.S. Turner, “*The Early Universe*”, Addison-Wesley Publishing Company, 1990.
- [23] T. S. Coleman and M. Roos, “Effective degrees of freedom during the radiation era,” Phys.

- Rev. D **68**, 027702 (2003) [astro-ph/0304281].
- [24] M. Cirelli and A. Strumia, “Minimal Dark Matter: Model and results,” New J. Phys. **11**, 105005 (2009) [arXiv:0903.3381 [hep-ph]].
 - [25] M. Ackermann *et al.* [Fermi-LAT Collaboration], “Constraining Dark Matter Models from a Combined Analysis of Milky Way Satellites with the Fermi Large Area Telescope,” Phys. Rev. Lett. **107**, 241302 (2011) arXiv:1108.3546 [astro-ph.HE].
 - [26] G. Jungman, M. Kamionkowski and K. Griest, “Supersymmetric dark matter,” Phys. Rept. **267**, 195 (1996) [arXiv:hep-ph/9506380].
 - [27] N. Arkani-Hamed, D. P. Finkbeiner, T. R. Slatyer and N. Weiner, Phys. Rev. D **79**, 015014 (2009) [arXiv:0810.0713 [hep-ph]].
 - [28] A. D. Sakharov, “Interaction Of An Electron And Positron In Pair Production,” Zh. Eksp. Teor. Fiz. **18**, 631 (1948) [Sov. Phys. Usp. **34**, 375 (1991)].
 - [29] J. L. Feng, M. Kaplinghat and H. -B. Yu, “Sommerfeld Enhancements for Thermal Relic Dark Matter,” Phys. Rev. D **82**, 083525 (2010) [arXiv:1005.4678 [hep-ph]]; S. Cassel, “Sommerfeld factor for arbitrary partial wave processes,” J. Phys. G **37**, 105009 (2010) [arXiv:0903.5307 [hep-ph]]; T. R. Slatyer, “The Sommerfeld enhancement for dark matter with an excited state,” JCAP **1002**, 028 (2010) [arXiv:0910.5713 [hep-ph]].
 - [30] A. Strumia, Nucl. Phys. B **809**, 308 (2009) [arXiv:0806.1630 [hep-ph]].
 - [31] C. -K. Chua, Phys. Rev. D **78**, 076002 (2008) [arXiv:0712.4187 [hep-ph]].
 - [32] H. -C. Tsai and K. -C. Yang, “Dark Matter Mass Constrained by the Relic Abundance, Direct Detections, and Colliders,” arXiv:1301.4186 [hep-ph].
 - [33] K. Griest and D. Seckel, “Three exceptions in the calculation of relic abundances,” Phys. Rev. D **43**, 3191 (1991).
 - [34] E. Aprile *et al.* [XENON100 Collaboration], “Dark Matter Results from 225 Live Days of XENON100 Data,” Phys. Rev. Lett. **109**, 181301 (2012) [arXiv:1207.5988 [astro-ph.CO]].
 - [35] K. -m. Cheung, “Constraints on electron quark contact interactions and implications to models of leptoquarks and extra Z bosons,” Phys. Lett. B **517**, 167 (2001) [hep-ph/0106251].